Dalton Transactions

ROYAL SOCIETY OF CHEMISTRY

PAPER

View Article Online
View Journal | View Issue

Cite this: *Dalton Trans.*, 2023, **52**, 9238

Oxychloridoselenites(IV) with cubane-derived anions and stepwise chlorine-to-oxygen exchange†

Maxime A. Bonnin and Claus Feldmann *

Received 12th May 2023,
Accepted 12th June 2023

DOI: 10.1039/d3dt01424j

rsc.li/dalton

The novel oxychloridoselenites(IV) [BMIm][Se_3Cl_{13}] (**1**), [BMIm][$Se_4Cl_{15}O$] (**2**), [BMIm]$_2$[$Se_4Cl_{14}O_2$] (**3**), [BMPyr]$_2$[$Se_4Cl_{14}O_2$] (**4**), [BMPyr]$_2$[$Se_6Cl_{18}O_4$] (**5**), [BMIm]$_2$[$SeCl_4O$] (**6**), [BMPyr]$_2$[$Se_2Cl_6O_2$] (**7**), and [BMPyr]$_2$[$Se_6Cl_{14}O_6$] (**8**) are prepared by ionic-liquid-based synthesis. Accordingly, $SeCl_4$, SeO_2 (**1–6**), and/or $SeOCl_2$ (**7**,**8**) as the starting materials are reacted in [BMIm]Cl or [BMPyr]Cl as ionic liquid (BMIm: 1-butyl-3-methylimidazolium, BMPyr: 1-butyl-1-methylpyrrolidinium; partially with $AlCl_3$ in addition). Generally, the composition and structure of title compounds can be derived from the tetrameric, hetero-cubane-type $(SeCl_4)_4$ as the initial building unit. Thus, chlorine is successively exchanged by oxygen from **1** to **8**. Moreover, the four edge-sharing ($SeCl_6$) octahedra in $(SeCl_4)_4$ are increasingly dismantled, ending with a $[SeCl_4O]^{2-}$ anion as a single pseudo-octahedron in **6**. Based on the weakly coordinating ionic liquid, it is possible to selectively obtain the different species *via* synthesis near room temperature (20–80 °C). The oxychloridoselenite anions $[Se_4Cl_{15}O]^-$, $[Se_4Cl_{14}O_2]^{2-}$, $[Se_6Cl_{18}O_4]^{2-}$, and $[Se_6Cl_{14}O_6]^{2-}$ are obtained for the first time. The title compounds are characterized by X-ray structure analysis based on single crystals and powders as well as by infrared spectroscopy and thermal analysis.

Introduction

Low-temperature syntheses near room temperature (≤100 °C) often have the limitation of the solvent influencing or even dominating the chemistry and composition of the reaction products.[1] On the one hand, the dissolution of the polar starting materials is usually driven by the formation of coordination complexes of cations and solvent molecules (*e.g.*, H_2O, THF, ethylene diamine).[1,2] As a result, solvent molecules often remain coordinated in the product. On the other hand, solvents can initiate redox reactions or acid–base reactions with the starting materials, limiting the electrochemical window or pH range in which a reaction can be performed (*e.g.*, H_2O, *lq*-NH_3, *lq*-SO_2).[1,2] Non-coordinating and chemically inert solvents (*e.g.*, heptane, toluene), however, often do not lead to any reaction at all due to the insolubility of polar starting materials and products. In this regard, ionic liquids have turned out to be a most effective alternative.[3] They offer high chemical and thermal stability in combination with good solubility and weakly coordinating properties.[4]

Due to the good solubility of many compounds at moderate temperatures (≤100 °C) and due to their inertness, ionic liquids also offer the option for fine-tuning reactions and obtaining metastable products with comparable composition and structure as well as only slightly different stability. Moreover, a series of compounds with unusual binding situations and/or spectacular building units was described, for instance, including cluster compounds, polyhalides, or new element modifications.[5] However, systematic studies on small changes in synthesis parameters and their influence on the obtained reaction product are limited to date. Examples comprise the formation of polybromides,[6] low-valent halides in the system Te–Bi/Al–Cl,[7] the connectivity of ($ZnBr_4$) tetrahedra in bromido zincates,[8] the structure of hexanuclear niobium clusters,[9] or the composition of chalcogenidometallates.[10] These reports mainly focus on halide compounds in ionic liquids, whereas studies on oxides are rare. This finding can be related to the higher lattice energy and the lower solubility of oxides in ionic liquids. Several studies, however, have already shown options to dissolve oxides in ionic liquids.[11]

Here, we address the reaction of $SeCl_4$, SeO_2 and/or $SeOCl_2$ in [BMIm]Cl or [BMPyr]Cl as the ionic liquid (BMIm: 1-butyl-3-methylimidazolium; BMPyr: 1-butyl-1-methylpyrrolidinium; partially with $AlCl_3$). The reactions were performed near room

Institute of Inorganic Chemistry (AOC), Karlsruhe Institute of Technology (KIT), Engesserstraße 15, D-76131 Karlsruhe, Germany. E-mail: claus.feldmann@kit.edu

†Electronic supplementary information (ESI) available: Additional data related to the analytical techniques and the unit cells of the title compounds **1–8**. CCDC 2259191 (**1**), 2259193 (**2**), 2259188 (**3**), 2259194 (**4**), 2259190 (**5**), 2259189 (**6**), 2259187 (**7**) and 2259192 (**8**). For ESI and crystallographic data in CIF or other electronic format see DOI: https://doi.org/10.1039/d3dt01424j

temperature (+20 to +80 °C) and resulted in the novel (oxy) chloridoselenites(IV) [BMIm][Se_3Cl_{13}] (**1**), [BMIm][$Se_4Cl_{15}O$] (**2**), [BMIm]$_2$[$Se_4Cl_{14}O_2$] (**3**), [BMPyr]$_2$[$Se_4Cl_{14}O_2$] (**4**), [BMPyr]$_2$[$Se_6Cl_{18}O_4$] (**5**), [BMIm]$_2$[$SeCl_4O$] (**6**), [BMPyr]$_2$[$Se_2Cl_6O_2$] (**7**), and [BMPyr]$_2$[$Se_6Cl_{14}O_6$] (**8**). The composition and structure of the title compounds can be derived from the tetrameric cubane-type $(SeCl_4)_4$[12] by stepwise chlorine-to-oxygen exchange.

Results and discussion

Ionic-liquid-based synthesis

The title compounds [BMIm][Se_3Cl_{13}] (**1**), [BMIm][$Se_4Cl_{15}O$] (**2**), [BMIm]$_2$[$Se_4Cl_{14}O_2$] (**3**), [BMPyr]$_2$[$Se_4Cl_{14}O_2$] (**4**), [BMPyr]$_2$[$Se_6Cl_{18}O_4$] (**5**), [BMIm]$_2$[$SeCl_4O$] (**6**), [BMPyr]$_2$[$Se_2Cl_6O_2$] (**7**), and [BMPyr]$_2$[$Se_6Cl_{14}O_6$] (**8**) were prepared by reaction of $SeCl_4$, SeO_2, and/or $SeOCl_2$ in [BMIm]Cl or [BMPyr]Cl as the ionic liquid (Fig. 1). The most important parameters to obtain one or other products comprise the temperature (+20 to +80 °C) and the ratio of the starting materials (Table 1). Here, it needs to be noted that the starting materials, except for $SeOCl_2$ (T_{melt}: 8.5 °C) but including [BMIm]Cl (T_{melt}: 70 °C) and [BMPyr]Cl (T_{melt}: 65 °C), are solid at room temperature. They only become liquid upon mixing or with moderate heating (Fig. 1). Subsequent to the reaction, the liquid phase usually shows an intense orange to red colour due to slight amounts of elemental selenium. After the removal of the ionic liquid, the title compounds were obtained as colourless, moisture-sensitive crystals.

The formation of the title compounds **1–8** can be ascribed to Lewis acid–base reactions. To this concern, the amphoteric features of chalcogen(IV) halides such as $SeCl_4$ are well-known.[13] Thus, $SeCl_4$ can serve as a Lewis base in the presence of strong Lewis acids, which we also used in previously studied reactions of $SeCl_4$ with $GaCl_3$, for instance, resulting in $[SeCl_3]^+[GaCl_4]^-$ with non-linear optic effects.[14] On the other hand, $SeCl_4$ can react as Lewis acid if a suitable Lewis base is present. Such behaviour is observed here with the stepwise chlorine-to-oxygen exchange, starting with the tetrameric cubane-like structure of $(SeCl_4)_4$.[12] In these reactions, the ionic liquid supports the dissolution of SeO_2 and serves as a weakly coordinating solvent.[3,4] Moreover, the presence of the voluminous cations of the ionic liquid promotes the formation of large oxychloridoselenite anions.

Whereas the compounds **1–6** were prepared by reaction of $SeCl_4$ and SeO_2 in [BMIm]Cl or [BMPyr]Cl (with the addition of $AlCl_3$ for **2** and **6**) as the ionic liquid, $SeOCl_2$ was used as additional starting material to obtain compounds **7** and **8** (Table 1). Since the title compounds have comparable composition, structure, and stability, small variations of temperature, stoichiometry, or Lewis acidity are the key to obtaining the one-or-other compound. Here, it needs to be noticed that the $SeCl_4$: SeO_2 ratio was varied between 5 : 1 and 1 : 3 with steps of ±1. At high amounts of $SeCl_4$ or SeO_2, however, only the respective starting material was observed to re-crystallize. All title compounds are obtained as colourless crystals (Fig. 1), which are highly sensitive to moisture. Thus, strict handling, including synthesis, storage and characterization, with inert conditions was necessary. All title compounds were obtained as phase-pure colourless crystals with a yield of 10–70%. The respective yield relates to the amount of larger crystals and mainly depends on the solubility of the respective starting materials and products in the ionic liquid. Composition, structure, and purity were confirmed by X-ray powder diffraction (XRD) (ESI: Fig. S1†) as well as by Fourier-transform infrared (FT-IR) spectroscopy and thermogravimetry (TG).

Structural characterization

From a more general perspective, all title compounds can be derived from the tetrameric, heterocubane-type $(SeCl_4)_4$ as the initial structure.[12] Starting with $(SeCl_4)_4$, on the one hand,

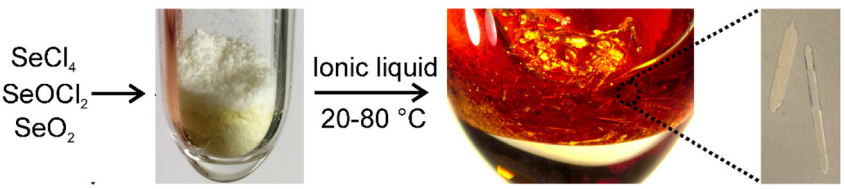

Fig. 1 Illustration of the general reaction of $SeCl_4$, $SeOCl_2$, SeO_2 in ionic liquids ([BMIm]Cl, [BMPyr]Cl, $AlCl_3$) near room temperature to obtain the title compounds **1–8** (exemplary photos shown for the synthesis of **2**).

Table 1 Conditions of synthesis for **1–8**

Compound	**1**	**2**	**3**	**4**	**5**	**6**	**7**	**8**
T/°C	50	50	80	80	50	25	50	25
$SeCl_4$: SeO_2	3 : 1	3 : 1	3 : 1	3 : 1	2 : 1	0 : 3	—	1 : 1
$SeCl_4$: $SeOCl_2$	—	—	—	—	—	—	0 : 1	1 : 1
$AlCl_3$	—	+	—	—	—	+	—	—
IL cation	$[BMIm]^+$	$[BMIm]^+$	$[BMIm]^+$	$[BMPyr]^+$	$[BMPyr]^+$	$[BMIm]^+$	$[BMPyr]^+$	$[BMPyr]^+$

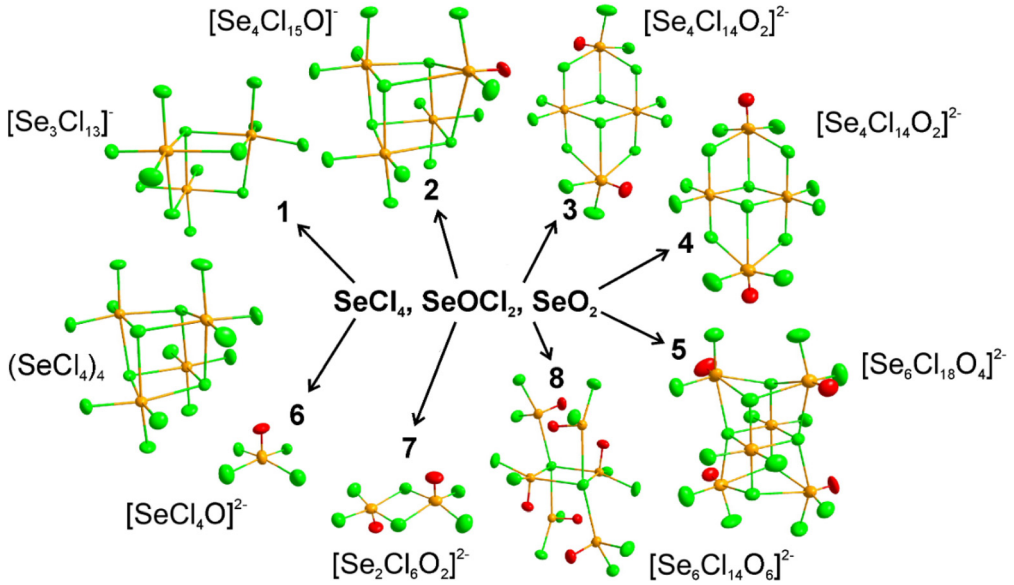

Fig. 2 Chemical and structural relation of the oxychloridoselenites(IV) in the title compounds **1**–**8** *via* chlorine-to-oxygen exchange and stepwise dismantling of the tetrameric cubane-type $(SeCl_4)_4$.

chlorine is exchanged by oxygen with increasing oxygen content from compound **1** to compound **8** (Fig. 2). On the other hand, the four edge-sharing ($SeCl_6$) octahedra in $(SeCl_4)_4$ are more and more dismantled, ending with the $[SeCl_4O]^{2-}$ anion as a single pseudo-octahedron in **6**. The structure of all compounds was determined based on single-crystal structure analysis (ESI: Table S1†). Space-group symmetry and structure were further validated by X-ray powder diffraction (XRD) with Rietveld analysis (ESI: Fig. S1†).

$[BMIm][Se_3Cl_{13}]$ (**1**) as the first compound crystallizes in the monoclinic, non-centrosymmetric space group $P2_1$ (ESI: Table S1, Fig. S2†) and consists of $[Se_3Cl_{13}]^-$ anions and $[BMIm]^+$ cations. The $[Se_3Cl_{13}]^-$ anion is established by three edge-sharing ($SeCl_6$) octahedra (Fig. 2), thus, with one ($SeCl_6$) octahedron missing in relation to the initial structure of $(SeCl_4)_4$. In fact, the $[Se_3Cl_{13}]^-$ anion is already known from $[Ph_3C][Se_3Cl_{13}]$.[15] **1** exhibits Se–Cl distances (216.5(4)–287.4(4) pm) and Cl–Se–Cl angles (84.3(1)–95.7(1)°) comparable to $[Ph_3C][Se_3Cl_{13}]$ (Se–Cl: 217.0(2)–281.0(2) pm; Cl–Se–Cl: 84.7(1)–96.0(1)°).[15] As expected, Se–Cl distances with bridging chlorine atoms are longer than for terminal chlorine atoms (Tables 2 and 3). Although present in the synthesis of **1**, it must be noted that SeO_2 is not involved in the product formation.

With similar conditions as for the synthesis of **1**, but with the addition of small amounts of $AlCl_3$, $[BMIm][Se_4Cl_{15}O]$ (**2**) was obtained, which crystallizes in the orthorhombic space group *Pbca* (ESI: Table S1, Fig. S3†). **2** consists of $[Se_4Cl_{15}O]^-$ anions and $[BMIm]^+$ cations. The $[Se_4Cl_{15}O]^-$ anion exhibits a cubane-like structure (Fig. 3a), which compares to the initial $(SeCl_4)_4$ by exchanging one terminal chlorine atom with oxygen (Fig. 2). The presence of oxygen leads to a significant distortion of the respective ($SeCl_5O$) octahedron in comparison to the initial ($SeCl_6$) octahedron. As a result, Se–Cl distances with selenium also bound to oxygen – indicated as Se* in the following – are longer as compared to those with selenium bound to chlorine only (Se*–Cl: 222.4(1)–327.1(1) pm; Se–Cl: 216.3(1)–284.2(1) pm) (Tables 2 and 3). The Se–Cl distances and Cl–Se–Cl angles (83.5(1)–95.5(1)°) are in accordance with literature data ($[Ph_3C][Se_3Cl_{13}]$: Se–Cl: 217.0(2)–281.0(2) pm; Cl–Se–Cl: 84.7(1)–96.0(1)°).[15] The Se*–O distance (161.9(2) pm) is also in accordance with the literature ($[n\text{-}Pr_4N]_2[Se_2Cl_6O_2]$: Se*–O with 159.3(9) pm).[16] In comparison to **1**, the presence of oxygen in **2** indicates that SeO_2 is now involved in the reaction, which can be ascribed to the presence of $AlCl_3$ as a Lewis acid. A cubane-derived oxychloridoselenite like in **2** – to the best of our knowledge – is unknown. Thus, only mono- and binuclear oxychloridoselenites were reported until now (*e.g.* $[Se_2Cl_7O_2]^-$).[17]

Upon increasing the reaction temperature to 80 °C, $[BMIm]_2[Se_4Cl_{14}O_2]$ (**3**) was obtained, which crystallizes in the monoclinic space group $P2_1/n$ (ESI: Table S1, Fig. S4†). Again, the structure of the $[Se_4Cl_{14}O_2]^{2-}$ anion can be derived from $(SeCl_4)_4$. Due to the high polarity of oxygen and the resulting distortion of the ($SeCl_5O$) building unit, the second ($SeCl_5O$) building unit is located opposite to the first so that an anion with two central edge-sharing ($SeCl_6$) octahedra and two double edge-sharing ($SeCl_5O$) on opposite sides was formed (Fig. 3b). The Se–Cl distances (218.5(1)–274.4(1) pm) are again in accordance with the literature ($[Et_4N][Se_2Cl_{10}]$: Se–Cl: 224.5–273.7 pm).[18] The Cl–Se–Cl angles (84.5(1)–95.0(1)°) point to the distortion of the octahedral building units (Tables 2 and 3). The Se*–Cl distances (221.3(2)–320.1(2) pm) and Cl–Se*–Cl/O angles (69.3(1)–103.5(2)°), as expected, indicate an even stronger distortion, as observed for **2**. Finally, the Se*–O distance is 162.2(4) pm ($[n\text{-}pr_4N]_2[Se_2Cl_6O_2]$: Se*–O: 159.3(9) pm).[16]

Based on similar conditions as for **3** but with [BMPyr]Cl instead of [BMIm]Cl, $[BMPyr]_2[Se_4Cl_{14}O_2]$ (**4**) was obtained.

Table 2 Selected distances (pm) in the title compounds **1**–**8** (Se*: Se atom with Se–O bond)

Compound	**1**	**2**	**3**	**4**	**5**	**6**	**7**	**8**
μ_1-Se–Cl	216.5(4)–223.0(4)	216.3(1)–221.4(1)	218.5(1)–222.0(1)	219.3(2)–222.1(2)	218.0(1)–219.8(1)	—	—	—
μ_2-Se–Cl	262.6(4)–272.7(4)	—	238.2(1)–238.4(1)	235.0(2)–241.4(2)	—	—	—	—
μ_3-Se–Cl	273.5(4)–287.4(4)	265.0(1)–284.2(1)	267.7(1)–274.4(1)	266.9(1)–274.3(2)	235.8(1)–244.4(1)	—	—	—
μ_4-Se–Cl	—	—	—	—	275.8(1)–288.0(1)	—	—	—
μ_1-Se*–Cl	—	222.4(1)–222.8(1)	221.3(2)–221.5(2)	217.4(2)–220.4(2)	221.6(2)–227.1(13)	242.7(1)–252.2(1)	231.4(2)–232.6(2)	220.4(1)–226.3(1)
μ_2-Se*–Cl	—	—	305.1(1)–320.1(2)	325.3(2)–334.5(2)	—	—	284.7(2)–287.7(2)	—
μ_3-Se*–Cl	—	301.9(1)–327.1(1)	320.1(1)	304.8(2)	316.0(2)–349.7(2)	—	—	—
μ_4-Se*–Cl	—	—	—	—	308.2(3)–315.8(3)	—	—	285.2(1)–288.9(1)
μ_1-Se*–O	—	161.9(2)	162.2(4)	165.4(5)	159.8(16)–160.5(3)	173.0(1)	162.0(5)	158.8(3)–160.1(2)

The composition and structure of **4** are very comparable to **3**. Thus, the space group ($P2_1/n$) and sum composition of the oxychloridoselenite anion ($[Se_4Cl_{14}O_2]^{2-}$) are identical (ESI: Table S1, Fig. S5†). Nevertheless, the location of the oxygen atoms is different. Whereas the oxygen atoms of $[Se_4Cl_{14}O_2]^{2-}$ in **3** are both in an axial position (in relation to the heterocubane), the oxygen atoms of $[Se_4Cl_{14}O_2]^{2-}$ in **4** are located in an equatorial position (in relation to the heterocubane) (Fig. 3c). For both cases, the ($SeCl_5O$) units are located on opposite sides of the central (Se_2Cl_{10}) unit. The different axial or equatorial locations can be ascribed to the interaction with the respective cation in **3** ($[BMIm]^+$) and **4** ($[BMPyr]^+$) and the formation of hydrogen bonding with C–H···O distances <280 pm (**3** with C–H···O: 259.7(5)–272.9(4) pm; **4** with C–H···O: 269.4 (5)–279.2(4) pm) (ESI: Fig. S6†).[19] The Se–Cl distances and Cl–Se–Cl angles in **4** (219.3(2)–274.3(2) pm, 84.5(1)–95.3(1)°), the Se*–Cl distances and Cl–Se*–Cl/O angles (217.4(2)–334.5(2) pm, 66.9(1)–104.4(2)°) as well as the Se–O distance (165.4(5) pm) are similar to **3** (Tables 2 and 3).

When decreasing the $SeCl_4 : SeO_2$ ratio to 2 : 1 (Table 1), $[BMPyr]_2[Se_6Cl_{18}O_4]$ (**5**) was obtained, crystallizing in the triclinic space group $P\bar{1}$ (ESI: Table S1, Fig. S7†). The $[Se_6Cl_{18}O_4]^{2-}$ anion in **5** also consists of a central (Se_2Cl_{10}) unit. In contrast to **3** and **4**, however, ($SeCl_5O$) octahedra are now attached on all four sides of this (Se_2Cl_{10}) unit (Fig. 3d), which results in a doubled-heterocubane-like structure. Distances and angles are comparable to **3** and **4**, including Se–Cl distances (218.0(1)–288.0(1) pm), Cl–Se–Cl angles (84.8(1)–96.6(1)°), Se*–Cl distances (221.6(2)–349.7(2) pm), Cl–Se*–Cl/O (67.2(1)–106.7(2)°) and Se–O distances (159.8(16)–160.5(3) pm) (Tables 2 and 3). Finally, it should be noticed that one oxygen atom turned out to be distorted. This was tackled by split atom positions and occupation with oxygen and chlorine of 50% for both.

In the absence of $SeCl_4$ and with the addition of $AlCl_3$ to activate SeO_2 (Table 1), $[BMIm]_2[SeCl_4O]$ (**6**) was obtained (space group $P1$, ESI: Table S1, Fig. S8†), which consists of pseudo-octahedral $[SeCl_4O]^{2-}$ anions and $[BMIm]^+$ cations (Fig. 4a). Thus, the Se : O ratio was increased to 1 : 1 with only a single pseudo-octahedral building unit remaining. Notably, **6** crystallizes in a polar, chiral space group without any inversion symmetry. The absence of centers of inversion can be illustrated by a (2 × 2 × 2) supercell, showing a unidirectional alignment of all $[SeCl_4O]^{2-}$ anions (ESI: Fig. S9†). Similar to $[Se_3Cl_{13}]^-$ in **1**, the $[SeCl_4O]^{2-}$ anion is known (*e.g.* in $[C_4H_{10}NO][SeCl_4O]$)[20] and exhibits comparable distances (**6**: Se*–Cl with 242.7(1)–252.2(1) pm, Se*–O distance with 173.0(1) pm *versus* 227.8(2)–277.6(2) pm and 160.8(4) pm in $[C_4H_{10}NO][SeCl_4O]$) (Tables 2 and 3). In fact, the Se*–O distance in **6** is more comparable with SeO_2 (162.3(1)–179.3(1)),[21] which is due to the presence of infinite chains of distorted, corner-sharing octahedra in $[C_4H_{10}NO][SeCl_4O]$, whereas the $[SeCl_4O]^{2-}$ anion in **6** is isolated.

Besides the variation of temperature and $SeCl_4 : SeO_2$ ratio, finally, $SeOCl_2$ was introduced as a starting material in the synthesis of compounds **7** and **8** (Table 1). Using $SeOCl_2$

Table 3 Angles (°) of the title compounds **1–8** (Se*: Se atom with Se–O bond)

Compound	**1**	**2**	**3**	**4**	**5**	**6**	**7**	**8**
Cl–Se–Cl	84.3(1)–95.7(1)	83.5(1)–95.5(1)	84.5(1)–95.0(1)	84.5(1)–95.3(1)	84.8(1)–96.6(1)	—	—	—
Cl–Se*–Cl	—	72.5(1)–95.1(1)	69.3(1)–95.4(1)	66.9(1)–99.4(1)	67.2(1)–106.7(3)	88.8(2)–90.8(2)	85.3(1)–92.2(1)	86.2(1)–96.6(1)
Cl–Se*–O	—	91.5(1)–104.0(1)	92.7(2)–103.5(2)	94.9(2)–104.4(2)	93.0(1)–106.4(7)	92.6(3)–98.3(3)	93.9(2)–101.3(2)	89.9(1)–103.1(1)

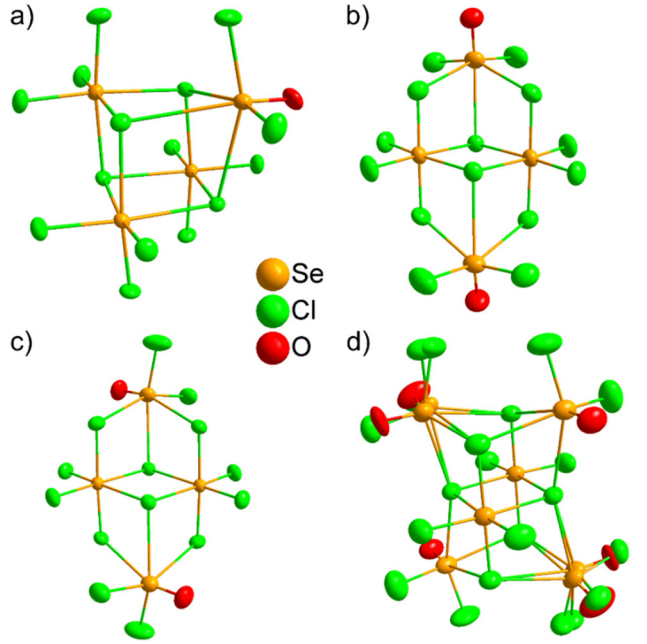

Fig. 3 Structure of oxychloridoselenite anions in (a) $[BMIm][Se_4Cl_{15}O]$ (**2**), (b) $[BMIm]_2[Se_4Cl_{14}O_2]$ (**3**), (c) $[BMPyr]_2[Se_4Cl_{14}O_2]$ (**4**), and (d) $[BMPyr]_2[Se_6Cl_{18}O_4]$ (**5**) (Cl/O partially disordered in **5**).

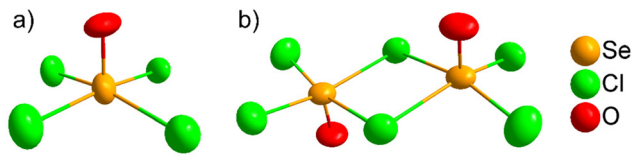

Fig. 4 Structure of oxychloridoselenite anions in (a) $[BMIm]_2[SeCl_4O]$ (**6**) and (b) $[BMPyr]_2[Se_2Cl_6O_2]$ (**7**).

as a starting material is an attractive alternative to SeO_2 since $SeOCl_2$ also introduces oxygen into the system and as it is more reactive as compared to SeO_2. The reaction of $SeOCl_2$ only in [BMPyr]Cl resulted in the formation of $[BMPyr]_2[Se_2Cl_6O_2]$ (**7**). **7** crystallizes in the triclinic space group $P\bar{1}$ (ESI: Table S1, Fig. S10†) and contains $[Se_2Cl_6O_2]^{2-}$ anions and $[BMPyr]^+$ cations. The anion consists of two edge-sharing ($SeCl_4O$) pseudo-octahedra (Fig. 4b) and is already described in $[PPh_4]_2[Se_2Cl_6O_2]$.[13] The Se*–Cl (231.4 (2)–287.7(2) pm) and the Se*–O distance (162.0(5) pm) are well in agreement with the literature ($[PPh_4]_2[Se_2Cl_6O_2]$: Se*–Cl with 226.6(2)–285.1(1) pm, Se*–O with 159.7(4) pm) (Tables 2 and 3).[13]

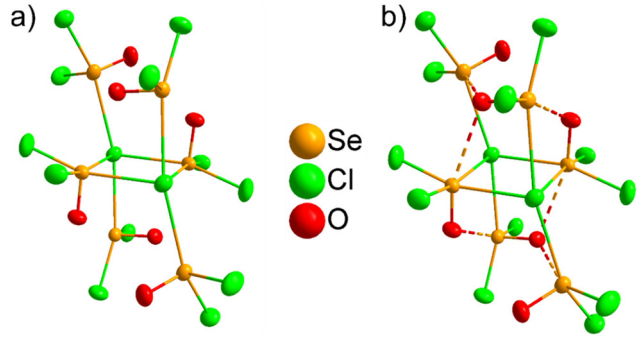

Fig. 5 Structure of oxychloridoselenite anion in $[BMPyr]_2[Se_6Cl_{14}O_6]$ (**8**) with (a) covalent bonds and (b) non-covalent interactions up to the sum of van der Waals radii.

Finally, the starting materials $SeCl_4$, $SeOCl_2$, and SeO_2 were combined in one reaction and resulted in $[BMPyr]_2[Se_6Cl_{14}O_6]$ (**8**) as a product. **8** crystallizes in the monoclinic space group $P2_1/n$ (ESI: Table S1, Fig. S11†) and consists of $[Se_6Cl_{14}O_6]^{2-}$ anions and $[BMPyr]^+$ cations. In relation to the structure of the initial $(SeCl_4)_4$, here, a central (Se_2Cl_2) ring remains (Fig. 5a). However, all selenium atoms are coordinated with oxygen and chlorine, resulting in six ($SeCl_3O$) building units, completed by additional partly longer-distance contacts to oxygen atoms to pseudo-octahedral arrangements (Fig. 5b). The Se*–Cl (220.4 (1)–288.9(1) pm) and Se*–O distances (158.8(3)–160.1(2) pm) are comparable to the literature data ($[Me_4N]_3[Se_2Cl_7O_2]Cl_2$: Se*–Cl with 230.5–279.4 pm, Se*–O with 160.9 pm).[9] The Cl–Se*–Cl (86.2(1)–96.6(1)°) and Cl–Se*–O angles (89.9(1)–103.1 (1)°) point to the distorted pseudo-octahedral coordination of selenium (Tables 2 and 3). Taking the sum of the van der Waals radii into account (Se: 190 pm, Cl: 175 pm, O: 152 pm),[21] additional non-covalent interactions occur with Se*···O distances of 274.0(3)–294.1(2) pm (sum of van der Waals radii: 342 pm),[21,22] in sum, resulting in pseudo-octahedral coordination of all Se atoms (Fig. 5b). In contrast, the even longer Se*···Cl distances (365.0(1)–371.5(1) pm) are above the sum of the van der Waals radii (365 pm).

Material properties

In addition to single-crystal structure analysis, the title compounds were examined by X-ray powder diffraction (XRD, ESI: Fig. S1†), Fourier-transform infrared (FT-IR) spectroscopy (Fig. 6), and thermal analysis (DTA/TG, ESI: Fig. S12 and S13†). Here, we have focused on the new compounds **2–5** and **8**. In the case of compounds **1**, **6**, and **7**, the specific combination of

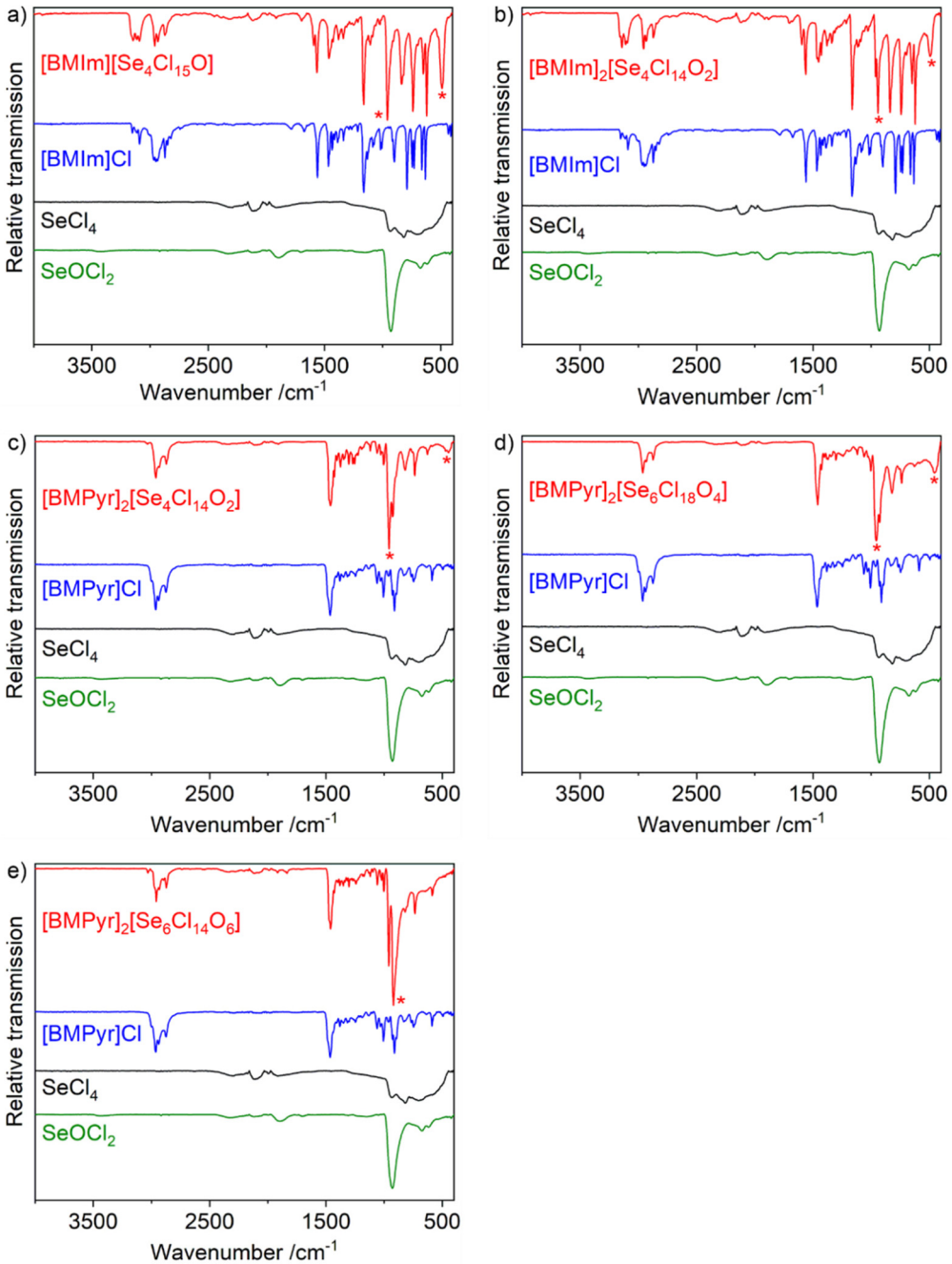

Fig. 6 FT-IR spectra of (a) $[BMIm][Se_4Cl_{15}O]$ (**2**), (b) $[BMIm]_2[Se_4Cl_{14}O_2]$ (**3**), (c) $[BMPyr]_2[Se_4Cl_{14}O_2]$ (**4**), (d) $[BMPyr]_2[Se_6Cl_{18}O_4]$ (**5**) and (e) $[BMPyr]_2[Se_6Cl_{14}O_6]$ (**8**) (ν(Se–O) and δ(Se–O) indicated by *; spectra of [BMIm]Cl, [BMPyr]Cl, $SeOCl_2$, $SeCl_4$ as references).

cation and anion is new as well, but the oxychloridoselenite anions were described before.

By comparison with the respective ionic liquid ([BMIm]Cl, [BMPyr]Cl), FT-IR spectra, first of all, indicate the vibrations of the $[BMIm]^+$ or $[BMPyr]^+$ cations (Fig. 6). Moreover, the absence of O–H or C=O vibrations shows the absence of typical impurities such as moisture and/or carbonates due to insufficient inert conditions. By comparison with the FT-IR spectra of $SeOCl_2$ and $SeCl_4$, the characteristic ν(Se–O) and δ(Se–O) vibrations at 1000–900 cm^{-1} and 500–400 cm^{-1} can be identified for the title compounds.[23] Specifically, ν(Se–O) occurs as a sharp, intense absorption with a wavenumber increasing with the number of oxygen atoms (Table 4). Moreover, the intensity of the ν(Se–O) vibration increases with the number of oxygen atoms in the respective oxychloridoselenite anion. In contrast to the ν(Se–O) and δ(Se–O) vibrations, the ν(Se–Cl) vibrations only sum up to a broad, non-specific absorption.

Table 4 Wavenumber (cm^{-1}) of ν(Se–O) and δ(Se–O) for the title compounds **2–5**, **8**

Compound	**2**	**3**	**4**	**5**	**8**
ν(Se–O)	958.7	941.2	958.5	956.6	960.5
δ(Se–O)	489.9	491.8	445.5	457.1	<430

Table 5 Evaluation of the TG data by comparing the experimentally observed weight loss with calculated data

	1st decomposition step/%		2nd decomposition step and remain/%	
Compound	Exp.	Calcd.	Exp	Calcd.
[BMIm][$Se_4Cl_{15}O$] (**2**)	85	*86*	15	*14*
[BMIm]$_2$[$Se_4Cl_{14}O_2$] (**3**)	84	*75*	16	*25*
[BMPyr]$_2$[$Se_4Cl_{14}O_2$] (**4**)	82	*75*	18	*25*
[BMPyr]$_2$[$Se_6Cl_{18}O_4$] (**5**)	84	*81*	16	*19*
[BMPyr]$_2$[$Se_6Cl_{14}O_6$] (**8**)	84	*79*	16	*21*

Thermal analysis with thermogravimetry (TG) shows a two-step decomposition with only slightly different values for the compounds **2–5** and **8** (ESI: Fig. S12†). The first decomposition step at 100–300 °C can be related to the decomposition and sublimation of $SeCl_4$ and $SeOCl_2$ (Table 5). The second decomposition step relates to a fragmentation of [BMIm]Cl and [BMPyr]Cl. Since TG was performed in a nitrogen atmosphere, the organic cations cannot be oxidized, so that amorphous carbon remains as a solid residue. Indeed, the crucibles were covered with an amorphous deep black film after TG analysis. Finally, differential thermal analysis (DTA) indicates the melting point of **3**, **4**, **5** at 70–80 °C, whereas **2** and **8** obviously decompose prior to melting (ESI: Fig. S13†). Taken together, X-ray diffraction based on single crystals and powders as well as FT-IR and TG confirm the composition and purity of the title compounds.

Conclusions

[BMIm][Se_3Cl_{13}] (**1**), [BMIm][$Se_4Cl_{15}O$] (**2**), [BMIm]$_2$[$Se_4Cl_{14}O_2$] (**3**), [BMPyr]$_2$[$Se_4Cl_{14}O_2$] (**4**), [BMPyr]$_2$[$Se_6Cl_{18}O_4$] (**5**), [BMIm]$_2$[$SeCl_4O$] (**6**), [BMPyr]$_2$[$Se_2Cl_6O_2$] (**7**) and [BMPyr]$_2$[$Se_6Cl_{14}O_6$] (**8**) are presented as novel oxychloridoselenites(IV). All compounds were prepared in ionic liquids ([BMIm]Cl, [BMPyr]Cl, partially with $AlCl_3$) with $SeCl_4$, SeO_2, and/or $SeOCl_2$ as the starting materials near room temperature (20–80 °C). The composition and structure of the oxychloridoselenite anions can be derived from the tetrameric, heterocubane-type $(SeCl_4)_4$. On the one hand, chlorine was successively exchanged by oxygen, and the Se : O ratio decreased from 4 : 1 to 1 : 1. On the other hand, the number of edge-sharing octahedra was reduced from 4 to 0. Besides crystal-structure analysis, the increased oxygen content can also be followed by infrared spectroscopy based on the wavenumber and intensity of the Se–O valence vibration. The oxychloridoselenite anions $[Se_4Cl_{15}O]^-$, $[Se_4Cl_{14}O_2]^{2-}$, $[Se_6Cl_{18}O_4]^{2-}$, and $[Se_6Cl_{14}O_6]^{2-}$ are generally obtained for the first time.

All compounds are of similar stability and prepared in a narrow temperature range. Temperature and ratio of starting materials are the main parameters to realize the one or other title compound. The ionic-liquid-based synthesis offers the option to perform reactions near room temperature in a weakly coordinating solvent so that the reaction and products are not dominated by the coordination and/or redox chemistry of the solvent. Such synthesis conditions, of course, offer the option to realize many additional metastable and new compounds.

Experimental methods

General considerations

Starting materials. The starting materials selenium(IV) oxide (SeO_2, 99.999%, Sigma-Aldrich), selenium(IV) chloride ($SeCl_4$, 99.9% Sigma-Aldrich), selenium(IV) oxychloride ($SeOCl_2$, 97.0%, Sigma-Aldrich) and aluminum(III) chloride ($AlCl_3$, 99.999%, Sigma-Aldrich) were commercially available and used without further purification. 1-Butyl-3-methylimidazolium chloride ([BMIm]Cl, 99.0%, Iolitec) and 1-butyl-1-methylpyrrolidium chloride ([BMPyr]Cl, 99.0%, Iolitec) were dried three days under reduced pressure (<10^{-3} mbar) at 120 °C before use.

Sample handling. All reactants were used and stored in Argon gloveboxes (MBraun Unilab, O_2/H_2O <1 ppm). Standard Schlenk-techniques were used for all reactions. Glass ampoules were evacuated (<10^{-3} mbar), heated, and flushed with argon three times to remove moisture.

Synthesis

[BMIm][Se_3Cl_{13}] (1). 50.0 mg (0.45 mmol) of selenium(IV) oxide, 298.7 mg (1.35 mmol) of selenium(IV) chloride and 157.4 mg (0.90 mmol) of [BMIm]Cl were reacted at 50 °C for 7 d. After cooling to room temperature with a rate of 1 K h^{-1}, colourless crystals were obtained with a yield of about 30%.

[BMIm][$Se_4Cl_{15}O$] (2). 25.0 mg (0.23 mmol) of selenium(IV) oxide, 149.2 mg (0.68 mmol) of selenium(IV) chloride, 15.0 mg (0.11 mmol) of aluminium(III) chloride and 78.7 mg (0.45 mmol) of [BMIm]Cl were reacted at 50 °C for 7 d. After cooling to room temperature with a rate of 1 K h^{-1}, colourless crystals were obtained with a yield of about 40%.

[BMIm]$_2$[$Se_4Cl_{14}O_2$] (3). 50.0 mg (0.45 mmol) of selenium(IV) oxide, 298.7 mg (1.35 mmol) of selenium(IV) chloride and 157.4 mg (0.90 mmol) of [BMIm]Cl were reacted at 80 °C for 7 d. After cooling to room temperature with a rate of 1 K h^{-1}, colourless crystals were obtained with a yield of about 30%.

[BMPyr]$_2$[$Se_4Cl_{14}O_2$] (4). 50.0 mg (0.45 mmol) of selenium(IV) oxide, 298.7 mg (1.35 mmol) of selenium(IV) chloride and 160.3 mg (0.90 mmol) of [BMPyr]Cl were reacted at 80 °C for 7 d. After cooling to room temperature with a rate of 1 K h^{-1}, colourless crystals were obtained with a yield of about 70%.

$[BMPyr]_2[Se_6Cl_{18}O_4]$ (5). 50.0 mg (0.45 mmol) of selenium(IV) oxide, 199.0 mg (0.90 mmol) of selenium(IV) chloride and 80.1 mg (0.45 mmol) of [BMPyr]Cl were reacted at 50 °C for 7 d. After cooling to room temperature with a rate of 1 K h^{-1}, colorless crystals were obtained with a yield of about 50%.

$[BMIm]_2[SeCl_4O]$ (6). 75.0 mg (0.68 mmol) of selenium(IV) oxide, 30.0 mg (0.22 mmol) of aluminium(III) chloride and 78.8 mg (0.45 mmol) of [BMIm]Cl were reacted at room temperature for 21 d. Colorless crystals were obtained with an estimated yield of about 10%.

$[BMPyr]_2[Se_2Cl_6O_2]$ (7). 40 μL (97.2 mg, 0.59 mmol) of selenium(IV) oxychloride and 104.1 mg, (0.59 mmol) of [BMPyr]Cl were reacted at 50 °C for 7 d. After cooling to room temperature with a rate of 1 K h^{-1}, colourless crystals were obtained with a yield of about 60%.

$[BMPyr]_2[Se_6Cl_{14}O_6]$ (8). 50.0 mg (0.45 mmol) of selenium(IV) oxide, 99.5 mg (0.45 mmol) of selenium(IV) chloride, 31 μL (74.7 mg, 0.45 mmol) of selenium(IV) oxychloride were and 80.1 mg (0.45 mmol) of [BMPyr]Cl were reacted at room temperature for 21 d. Colourless crystals were obtained with a yield of about 70%.

Analytical characterization

X-ray data collection and structure solution. Selected single crystals of the title compounds were covered with inert oil (perfluorpolyalkylether, ABCR) and deposited on a micro gripper (MiTeGen). Data collection for **1** and **3–8** was performed at 213 K on an IPDS II image plate diffractometer (STOE) using Mo-K_α radiation (λ = 71.073 pm, graphite monochromator). Data collection for **2**, which was obtained with significantly smaller crystals, was performed at 180 K on an STOE StadiVari Diffractometer with Euler geometry (STOE) using Ga-K_α radiation (λ = 1.34013 Å, graded multilayer mirror as the monochromator). Data reduction and absorption correction were performed by the X-AREA software package (version 1.75, STOE) and STOE LANA (version 1.63.1, STOE).[24] For structure solution and refinement, SHELXT and SHELXL were used.[25] All non-hydrogen atoms were refined anisotropically. The positions of hydrogen atoms were modeled by idealized C–H bonds. Images were illustrated with DIAMOND.[26] Detailed crystallographic data are listed in the ESI (Table S1†). Further details related to the crystal structures may be obtained from the joint CCDC/FIZ Karlsruhe deposition service on quoting the depository numbers: 2259191 (**1**), 2259193 (**2**), 2259188 (**3**), 2259194 (**4**), 2259190 (**5**), 2259189 (**6**), 2259187 (**7**) and 2259192 (**8**).†

Conflicts of interest

The authors declare no competing financial interest.

Acknowledgements

The authors thank the Deutsche Forschungsgemeinschaft (DFG) for funding. Moreover, we acknowledge the Karlsruhe Nano Micro Facility (KNMF) and Prof. Dr D. Fenske and Dr A. Eichhöfer for the data collection on an STOE StadiVari diffractometer with a Ga-metal-jet source.

References

1 *Modern Inorganic Synthetic Chemistry*, ed. R. Xu and Y. Xu, Elsevier, Amsterdam, 2nd edn, 2017.
2 N. N. Greenwood and A. Earnshaw, *Chemistry of the Elements*, Butterworth-Heinemann, Oxford, 2nd edn, 1998.
3 P. Wasserscheid and T. Welton, *Ionic Liquids in Synthesis*, Wiley-VCH, Weinheim, 2008.
4 (*a*) T. Zhang, T. Doert, H. Wang, S. Zhang and M. Ruck, *Angew. Chem., Int. Ed.*, 2021, **60**, 22148–22165; (*b*) D. Freudenmann, S. Wolf, M. Wolff and C. Feldmann, *Angew. Chem., Int. Ed.*, 2011, **50**, 11050–11060.
5 (*a*) R. Brueckner, H. Haller, S. Steinhauer, C. Mueller and S. Riedel, *Angew. Chem., Int. Ed.*, 2015, **54**, 15579–15583; (*b*) M. Knies, M. Kaiser, A. Isaeva, U. Mueller, T. Doert and M. Ruck, *Chem. – Eur. J.*, 2018, **24**, 127–132; (*c*) C. Donsbach, K. Reiter, D. Sundholm, F. Weigend and S. Dehnen, *Angew. Chem., Int. Ed.*, 2018, **57**, 8770–8774; (*d*) K. Glootz, D. Himmel, D. Kratzert, B. Butschke, H. Scherer and I. Krossing, *Angew. Chem., Int. Ed.*, 2019, **58**, 14162–14166; (*e*) S. S. Rudel, H. L. Deubner, M. Mueller, A. J. Karttunen and F. Kraus, *Nat. Chem.*, 2020, **12**, 962–967; (*f*) E. Merzlyakova, S. Wolf, S. Lebedkin, L. Bayarjargal, B. L. Neumeier, D. Bartenbach, C. Holzer, W. Klopper, B. Winkler, M. Kappes and C. Feldmann, *J. Am. Chem. Soc.*, 2021, **143**, 798–804.
6 (*a*) M. E. Easton, A. J. Ward, T. Hudson, P. Turner, A. F. Masters and T. Maschmeyer, *Chem. – Eur. J.*, 2015, **21**, 2961–2965; (*b*) K. Sonnenberg, L. Mann, F. A. Redeker, B. Schmidt and S. Riedel, *Angew. Chem., Int. Ed.*, 2020, **59**, 5464–5493.
7 M. F. Groh, U. Mueller, E. Ahmed, A. Rothenberger and M. Ruck, *Z. Naturforsch., B: J. Chem. Sci.*, 2013, **68**, 1108–1122.
8 D. Hausmann and C. Feldmann, *Dalton Trans.*, 2013, **42**, 13487–13494.
9 D. H. Weiss, F. Schroeder and M. Koeckerling, *Z. Anorg. Allg. Chem.*, 2017, **643**, 345–351.
10 Z. Wu, G. Stuhrmann and S. Dehnen, *Chem. Commun.*, 2022, **58**, 11609–11624.
11 (*a*) P. Nockemann, B. Thijs, T. N. Parac-Vogt, K. Van Hecke, L. Van Meervelt, B. Tinant, I. Hartenbach, T. Schleid, V. T. Ngan, M. T. Nguyen and K. Binnemans, *Inorg. Chem.*, 2008, **47**, 9987–9999; (*b*) S. Wellens, N. R. Brooks, B. Thijs, L. Van Meervelt and K. Binnemans, *Dalton Trans.*, 2014, **43**, 3443–3452; (*c*) J. Richter and M. Ruck, *RSC Adv.*, 2019, **9**, 29699–29710.
12 R. Kniep, L. Korte and D. Mootz, *Z. Naturforsch., B: Anorg. Chem., Org. Chem.*, 1981, **36**, 1660–1662.
13 B. Krebs, A. Schäffer and M. Hucke, *Z. Naturforsch., B: Anorg. Chem., Org. Chem.*, 1982, **37**, 1410–1417.
14 M. A. Bonnin, L. Bayarjargal, V. Milman, B. Winkler and C. Feldmann, *Inorg. Chem. Front.*, 2023, **10**, 2636–2644.

15 F.-P. Ahlers, E. Lührs and B. Krebs, *Z. Anorg. Allg. Chem.*, 1991, **594**, 7–22.
16 M. A. James, O. Knop and T. S. Cameron, *Can. J. Chem.*, 1992, **70**, 1795–1821.
17 A. N. Usoltsev, N. A. Korobeynikov, B. A. Kolesov, A. S. Novikov, P. A. Abramov, M. N. Sokolov and S. A. Adonin, *Chem. – Eur. J.*, 2021, **27**, 9292–9294.
18 W. Czado, M. Maurer and U. Müller, *Z. Anorg. Allg. Chem.*, 1998, **624**, 1871–1876.
19 T. Steiner, *Crystallogr. Rev.*, 1996, **6**, 1–57.
20 S. Hasche, O. Reich, I. Beckmann and B. Krebs, *Z. Anorg. Allg. Chem.*, 1997, **623**, 724–734.
21 M. Mantina, A. C. Chamberlin, R. Valero, C. J. Cramer and D. G. Truhlar, *J. Phys. Chem. A*, 2009, **113**, 5806–5812.
22 K. Ståhl, *Z. Kristallogr.*, 1992, **202**, 99–108.
23 C. Feldmann and M. Jansen, *Chem. Ber.*, 1994, **127**, 2173–2176.
24 *X-RED,32, Data Reduction Program*, STOE, Darmstadt, 2001.
25 G. M. Sheldrick, SHELXT – Integrated space-group and crystal-structure determination, *Acta Crystallogr., Sect. A: Found. Adv.*, 2015, **71**, 3–8.
26 *DIAMOND, Crystal and Molecular Structure Visualization*, Crystal Impact GbR, Bonn, 2016.